

Resonant two-photon ionization spectra of van der Waals complexes: *o*-, *m*- and *p*-C₆H₄R₂...N₂ (R ≡ F, CH₃)

Yihua Hu¹, Wenyun Lu, Shihe Yang^{*}

Department of Chemistry, The Hong Kong University of Science and Technology, Clear Water Bay, Kowloon, Hong Kong

Abstract

The jet-cooled van der Waals (vdW) complexes *o*-, *m*- and *p*-C₆H₄R₂...N₂ were studied by the one-colour resonant two-photon ionization technique (R2PI) through the S₁ ← S₀ transition around the $\bar{\nu}_0^0$ band. N₂ in *o*-, *m*- and *p*-C₆H₄F₂...N₂ was found to rotate almost freely around an axis perpendicular to the benzene ring, whereas no such internal rotational features were observed for *o*-, *m*- and *p*-C₆H₄(CH₃)₂...N₂. All the vdW vibrational modes of the complexes studied were identified and assigned accordingly. For *p*-C₆H₄(CH₃)₂...N₂, Fermi resonance was observed between the CH₃ internal rotational levels and the vdW stretching motion of N₂ against the benzene ring. For all the complexes studied (*o*-, *m*- and *p*-C₆H₄R₂...N₂), irrespective of whether R ≡ F or CH₃, the $\bar{\nu}_0^0$ band shifts relative to the monomer origins 0₀⁰ were largest for the para-substituted complexes, least for the meta-substituted complexes and in between for the ortho-substituted complexes. © 1997 Elsevier Science S.A.

Keywords: R2PI spectra; Supersonic jet; van der Waals complex

1. Introduction

During the last two decades, many researchers have employed the technique of resonant two-photon ionization (R2PI) to investigate the van der Waals (vdW) interaction of rare gas atoms and small molecules with benzene and its derivatives [1–10]. From the R2PI spectra of vdW complexes, information on the complex structure, intermolecular vibrational frequencies in the excited states and electronic transition frequency shifts has been obtained. Attention has been paid in this type of complex to the effect of H substitution in the benzene ring by other atoms or groups on the vdW vibrations, electronic transitions, etc. Mons et al. [7] studied complexes of single-H-substituted benzene derivatives (BDs) (C₆H₅X; X ≡ F, Cl, CH₃, OH) and C₆H₅X...Ar. The following observations were found:

1. the electronic transition frequency shifts $\Delta\nu$ of these complexes relative to the monomer C₆H₅X possess a good linear relationship with the corresponding electronic transition frequency ν of C₆H₅X;
2. the stretching vibrational mode perpendicular to the benzene ring can be approximated by a diatomic model;

3. the bending vibrational frequencies perpendicular to the symmetry plane of the complexes are essentially unchanged.

The next natural question is: what would happen if we changed Ar to a small molecule M? Such a complex BD...M, apart from its intermolecular modes, has internal rotational degrees of freedom, and therefore the interaction is more complicated. To use BD...Ar as a reference, we selected BD...N₂ as an example for our studies, since diatomic N₂ possesses physical parameters similar to those of Ar (e.g. ionization potential, polarizability, dipole moment, etc.).

We have recently reported R2PI studies of the vdW complexes C₆H₅X...N₂ (X ≡ F, Cl, Br) [11]. By comparing the R2PI spectra of C₆H₅X...N₂ (X ≡ F, Cl) with those of C₆H₅X...Ar reported in Ref. [6], it is found that the vdW stretching and bending vibrations have a one-to-one correspondence. Further analysis of the vdW vibrational modes shows the following:

1. in much the same way as C₆H₅X...Ar, the stretching mode of C₆H₅X...N₂ can also be approximately described by a diatomic model;
2. the force constants of the stretching mode and the bending mode in the symmetry plane increase from C₆H₅F...N₂ to C₆H₅Cl...N₂, but the variation of the bending force constant in the symmetry plane is not monotonic;

^{*} Corresponding author.

¹ Present address: Department of Physics, Guangdong University of Technology, Guangzhou, People's Republic of China.

- for the internal rotation of N₂ in the complex C₆H₅X...N₂ around an axis perpendicular to the benzene ring, there exists only a small barrier of less than 10 cm⁻¹;
- the S₁ ← S₀ band origin 0₀⁰ is red shifted relative to the monomer; furthermore, the shifts from F to Br show a good linear relationship with the change in the dispersion interaction energy.

This paper investigates the effect of double H substitution on the R2PI spectra of *o*-, *m*- and *p*-C₆H₄R₂...N₂ (R ≡ F, CH₃). The complex structures, vibrational frequencies and transition frequency shifts are analysed.

2. Experimental details

The experimental apparatus has been described elsewhere [12]. Only a brief description is provided here. An N₂–Ar gas mixture (0.03 : 1) was bubbled through a glass container containing the liquid C₆H₄R₂ (R ≡ F, CH₃). The vapour of C₆H₄R₂ was carried by the N₂–Ar gas mixture and expanded through a 0.5 mm diameter exit hole of a pulsed nozzle. By adjusting the nozzle backing pressure and nozzle opening current, the formation of large vdW complexes (larger than C₆H₄R₂...N₂) could be minimized in order to reduce the effects of the fragmentation of larger clusters. The supersonic beam thus formed was collimated by a 2 mm diameter skimmer and directed into the detection region of a reflectron time-of-flight (RTOF) mass spectrometer. The source chamber and flight tube were differentially pumped by 10 in and 6 in diffusion pumps with water baffles respectively.

The complexes formed were two-photon ionized through resonance by pulsed radiation in the wavelength range 262–280 nm. This blue light was generated by doubling the dye laser output (coumarin 540A) with a BBOI crystal. The dye laser was pumped by an XeCl excimer laser (Lambda Physik LPX210i/LPD3002). The laser pulse energy used was 0.3–1.0 mJ. The laser linewidth of the excitation source was typically approximately 0.3 cm⁻¹.

The ionized vdW complexes were extracted by a high-voltage pulse, guided by a pair of horizontal and vertical deflection plates, focused by an Einzel lens, mass selected by a pulsed mass gate and reflected by an ion reflectron. The reflected ions were detected by a dual microchannel plate (MCP) detector. The mass gate was particularly useful in reducing the much stronger monomer ion signal intensities which would otherwise saturate the MCP detector. The MCP signal was preamplified by a preamplifier (Stanford 445), digitized by a 100 MHz transient recorder and processed by a 486 PC. All the timing pulses (DG535), dye laser scanning and data acquisition were controlled and carried out by the PC.

3. The conformations of C₆H₄R₂...N₂

For the vdW complexes C₆H₄R₂...N₂ (R ≡ F, CH₃), we are interested in the vdW conformations in which the two R

Table 1

Lennard–Jones potential parameters used in energy calculations of the complexes

	A (cm ⁻¹ Å ⁻¹²)	C (cm ⁻¹ Å ⁻⁶)
C–N	1.728×10^8	1.575×10^5
H–N	2.500×10^7	4.527×10^4
F–N	7.754×10^7	7.531×10^4

groups or atoms are located in the ortho, meta and para positions relative to each other. The Lennard–Jones empirical potential can provide a potential energy surface which is in accord with the experimental results. To consider the interaction between C₆H₄R₂ and N₂, we use the classical atomic interaction potential and assume that the interaction energy is the summation of all the atom–atom interaction energies. The atom–atom pair potential takes the form

$$V(r) = (A/r^{12}) - (C/r^6) + Q_1Q_2/r \quad (1)$$

In the process of energy minimization, the bond lengths and bond angles in N₂ and C₆H₄R₂ are fixed. The parameters A and C were obtained from the literature [13], and are listed in Table 1. The interaction parameter between the N atom and F atom is obtained from the geometric average of the self-interaction parameters of N and F. The partial charge distribution of C₆H₄R₂ was calculated using the GAUSSIAN 94 package at the HF/6-311G* level. The partial charge distribution of N₂ was taken from the literature [14].

The calculation of the minimum energy structure of C₆H₄R₂...N₂ (R ≡ F, CH₃) shows that the distance between the centre-of-mass (CM) of N₂ and the benzene ring is approximately 3.3 Å. When the two R groups are in the para positions, the CM of N₂ and the CM of *p*-C₆H₄R₂ are in the symmetry axis (Z axis) with the N₂ bond axis parallel to the X axis (see Fig. 1). When the two R groups are in the meta and ortho positions, the CM of N₂ is no longer in the Z axis with the CM of *m*- and *o*-C₆H₄R₂. When in the meta position, the CM of N₂ is 0.2 Å (for R ≡ F) and 0.1 Å (for R ≡ CH₃) away from the CM of *m*-C₆H₄R₂ in the X direction. The N₂ bond axis is parallel to the benzene ring and perpendicular to the symmetry plane ZOX. When in the ortho position, the distance between the two CMs is 0.5 Å (for R ≡ F) and 0.15 Å (for R ≡ CH₃) in the X direction. N₂ is in the symmetry plane ZOX and shows small angles with the X axis of 5° (for R ≡ F) and 3° (for R ≡ CH₃). For all three complexes in the equilibrium position, as N₂ rotates around an axis perpendicular to the benzene ring, the vdW interaction potential $U(\theta)$ changes by as little as 10–25 cm⁻¹. This suggests that the rotation of N₂ above the benzene ring is nearly free, in accord with the observed R2PI spectra.

Our previous experiments showed that the vdW stretching frequencies of C₆H₅X...N₂ (X ≡ F, Cl, Br) can be approximated by the diatomic model [11]. Therefore we used the vdW potential and diatomic model to estimate the vdW stretching frequency of C₆H₄R₂...N₂. In the diatomic model, the vdW stretching frequency is $\omega_s = (k_s/\mu)^{1/2}$. Here, μ is

the reduced mass of N_2 and $C_6H_4R_2$ (all of the three complexes have the same reduced mass) and k_s is the stretching force constant (the translation of N_2 along the Z direction). In order to calculate the stretching force constant, we fix the X , Y coordinates of N_2 in the equilibrium position, move N_2 by small steps and calculate the potential energy changes with the Lennard–Jones 6-12-1. By fitting the potential energy change to $U(Z) = U_0 + (1/2)k_s(\Delta Z)^2$, we obtain the vdW stretching force constant k_s . The calculation shows that the stretching force constants of all three complexes are nearly the same ($k_s = 2.45 \times 10^3 \text{ cm}^{-1} \text{ \AA}^{-2}$ for $R \equiv F$ and $2.80 \times 10^3 \text{ cm}^{-1} \text{ \AA}^{-2}$ for $R \equiv CH_3$). As a consequence, the vdW stretching frequencies of all three complexes are very similar (approximately 60 cm^{-1} , 64 cm^{-1}). This is consistent with the stretching frequencies ($53\text{--}54 \text{ cm}^{-1}$) observed for the three complexes ($R \equiv F, CH_3$).

4. Results and discussion

4.1. Spectral assignments

For vdW complexes of benzene and BDs with Ar, some information about the vdW vibrational characteristics is already known. For example, in vdW complexes of mono-substituted benzene with Ar, the bending vibrational frequency of Ar in the symmetry plane lies between 16 and 22 cm^{-1} , and the vdW stretching vibrational frequency is

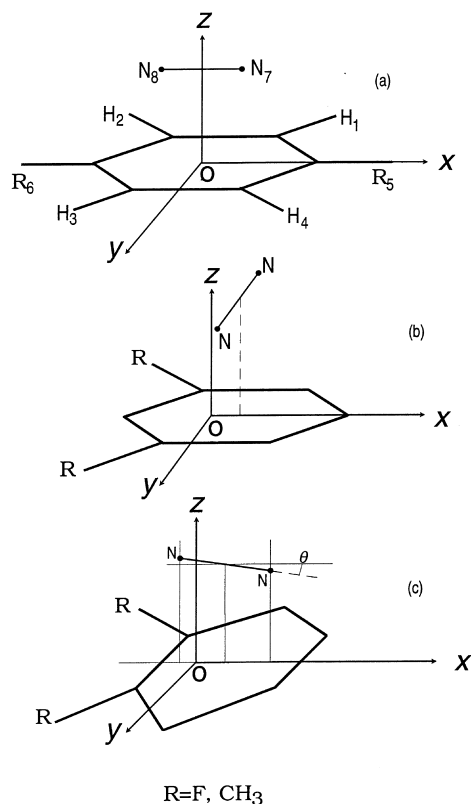


Fig. 1. Coordinate system of the calculated structure for the vdW complexes $C_6H_4R_2 \dots N_2$ ($R \equiv F, CH_3$).

roughly in the range $40\text{--}49 \text{ cm}^{-1}$ [6]. In contrast, much less is known at present about the intermolecular vibrations of vdW complexes of benzene and BDs with N_2 . Since $BD \dots N_2$ has two more intermolecular vibrational modes than $BD \dots Ar$, the spectra of $BD \dots N_2$ are more complicated. A case in point is the twisting motion of N_2 along an axis perpendicular to the benzene ring. It has only a small barrier, causing internal rotation. Many spectral lines stemming from this motion can be observed in R2PI experiments [1,9,10], making spectral assignments difficult.

For the vdW complex $C_6H_6 \dots N_2$, there have been several reports on its vdW vibrations. Ohshima et al. [15] obtained the centrifugal distortion constants by microwave spectroscopy. From the centrifugal distortion constants, they estimated the stretching vibration frequency of N_2 against the benzene ring to be 45.6 cm^{-1} , and the bending vibrational frequency of N_2 parallel to the benzene ring to be 25.6 cm^{-1} for the ground electronic state of $C_6H_6 \dots N_2$. Ref. [16] gives the calculated stretching vibrational frequency and twisting (t_y) vibrational frequency of $C_6H_6 \dots N_2$ in the ground electronic state as 53 cm^{-1} and 73 cm^{-1} respectively. Nowak et al. [1] obtained a vdW vibrationally resolved R2PI spectrum of $C_6H_6 \dots N_2$ through the $S_1 \leftarrow S_0$ transition. They attributed the peaks at $+23 \text{ cm}^{-1}$ and $+50 \text{ cm}^{-1}$ (relative to $\bar{0}_0^0$) to b_{x0}^2 and b_{x0}^4 respectively, the peak at $+37 \text{ cm}^{-1}$ to b_{y0}^2 and the peak at 65 cm^{-1} to the superposition of b_{y0}^4 and S_{20}^1 . The basis for this assignment is that the spectral transitions of $C_6H_6 \dots N_2$ should follow the selection rule of rigid molecules: for the two bending vibrations, $\Delta v = 0, \pm 2, \pm 4, \dots$, where v is the bending vibrational quantum number. However, recent high-resolution rotationally resolved spectra show that this type of vdW complex has rather strong Herzberg–Teller coupling between the vdW bending vibrations and the electronic states involved, allowing the fundamental bending vibrations to be observed. Consequently, the peak previously assigned to b_0^2 was reassigned to b_0^1 [17,18]. Stimulated Raman spectra of $C_6H_6 \dots Ar(N_2)$, $C_6H_5F \dots Ar$, $C_6H_5NH_2 \dots Ar$, etc. also exhibited the fundamental bending vibrations for the ground electronic states [19].

We have recently obtained the vdW vibrationally resolved spectra of $C_6H_5X \dots N_2$ ($X \equiv F, Cl, Br$) using the R2PI technique through the $S_1 \leftarrow S_0$ transition. It was found that the stretching and bending vibrations of $C_6H_5X \dots N_2$ show a good one-to-one correspondence with those of $C_6H_5X \dots Ar$. The bending fundamental vibration b_{x0}^1 of $C_6H_5X \dots N_2$ in the symmetry plane was found to have a frequency of $+20.7 \text{ cm}^{-1}$ for $X \equiv F$, $+16.0 \text{ cm}^{-1}$ for $X \equiv Cl$ and $+15.4 \text{ cm}^{-1}$ for $X \equiv Br$. Referring to the stimulated Raman spectra of $C_6H_6 \dots Ar(N_2)$ and $C_6H_5F \dots Ar$ [19], the fundamental bending vibration of $C_6H_5X \dots N_2$ perpendicular to the symmetry plane was assigned to the peak at $+39.6 \text{ cm}^{-1}$ ($X \equiv F$) and to the peak at $+31.5 \text{ cm}^{-1}$ ($X \equiv Cl$). The peaks at $+49.8 \text{ cm}^{-1}$ ($X \equiv F$) and $+49.3 \text{ cm}^{-1}$ ($X \equiv Cl$) were assigned to the stretching vibrations S_0^1 of $C_6H_5X \dots N_2$ ($X \equiv F, Cl$). The peak at $+65 \text{ cm}^{-1}$ was assigned to the fundamental twisting vibration t_{y0}^1 . Since the vdW vibrational frequencies are not

expected to change significantly from $C_6H_6...N_2$ to $C_6H_5F...N_2$, we believe that the spectral lines at $+23\text{ cm}^{-1}$, $+37\text{ cm}^{-1}$, $+50\text{ cm}^{-1}$ and $+65\text{ cm}^{-1}$ of $C_6H_6...N_2$ belong to b_{x0}^1 , b_{y0}^1 , S_{z0}^1 and t_{y0}^1 respectively. Combining the above discussion with relevant theories, we attempt to discuss the assignment of the R2PI spectra of $C_6H_4R_2...N_2$ ($R \equiv F, CH_3$) shown in Figs. 2–7.

The $S_1 \leftarrow S_0 0_0^0$ band of the monomers *o*-, *m*- and *p*- $C_6H_4R_2$ ($R \equiv F, CH_3$) lies in the frequency range $36\,700$ – $37\,950\text{ cm}^{-1}$ [20–22]. The 0_0^0 transition frequencies are: $37\,909\text{ cm}^{-1}$ (*o*- $C_6H_4F_2$), $37\,824\text{ cm}^{-1}$ (*m*- $C_6H_4F_2$), $36\,838\text{ cm}^{-1}$ (*p*- $C_6H_4F_2$), $37\,313.3\text{ cm}^{-1}$ (*o*- $C_6H_4(CH_3)_2$), $36\,956.3\text{ cm}^{-1}$ (*m*- $C_6H_4(CH_3)_2$) and $36\,732.8\text{ cm}^{-1}$ (*p*- $C_6H_4(CH_3)_2$). All the above molecules, except *p*- $C_6H_4F_2$, can be probed by the one-colour R2PI technique to obtain the 0_0^0 band excitation spectra. For *p*- $C_6H_4F_2$, the two-photon energy of the $S_1 \leftarrow S_0 0_0^0$ band transition is lower than the ionization threshold ($73\,871\text{ cm}^{-1}$) by 195 cm^{-1} ; therefore its one-colour R2PI spectrum cannot be observed. In order to investigate the vdW vibrations of $C_6H_4R_2...N_2$ ($R \equiv F, CH_3$), all the vdW complexes of the above molecules with N_2 , except *p*- $C_6H_4F_2...N_2$, were studied based on the vibrationally resolved spectra near 0_0^0 . For *p*- $C_6H_4F_2...N_2$, since there is no other transition near 30_0^2 ($+240\text{ cm}^{-1}$) for the monomer, we chose the region near 30_0^2 to investigate the complex vdW vibrations.

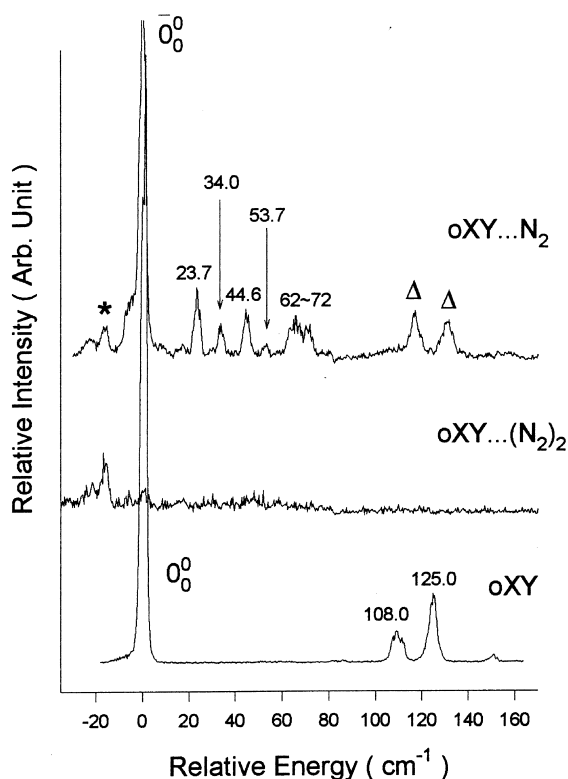


Fig. 2. R2PI spectra of *o*- $C_6H_4(CH_3)_2...N_2$, *o*- $C_6H_4(CH_3)_2...(N_2)_2$ and *o*- $C_6H_4(CH_3)_2$ in the vicinity of the $S_1 \leftarrow S_0 0_0^0$ band. The spectra of *o*- $C_6H_4(CH_3)_2...N_2$ and *o*- $C_6H_4(CH_3)_2...(N_2)_2$ have the same frequency scale.

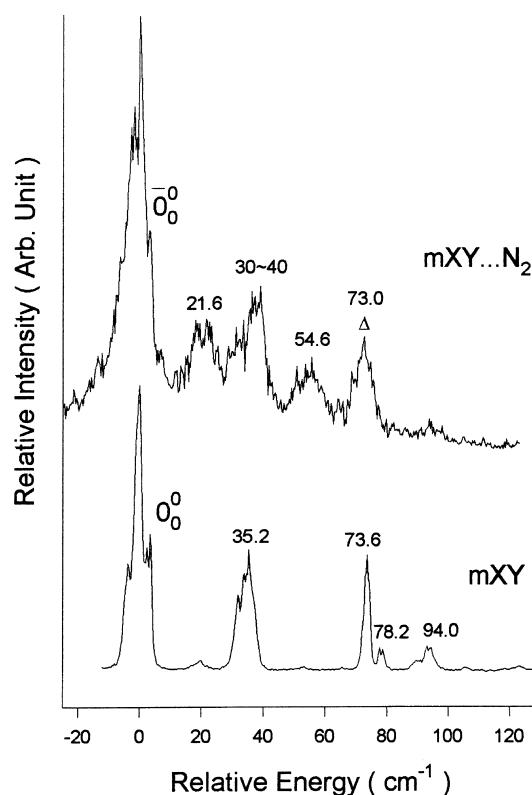


Fig. 3. R2PI spectra of *m*- $C_6H_4(CH_3)_2...N_2$ and *m*- $C_6H_4(CH_3)_2$ in the vicinity of the $S_1 \leftarrow S_0 0_0^0$ band.

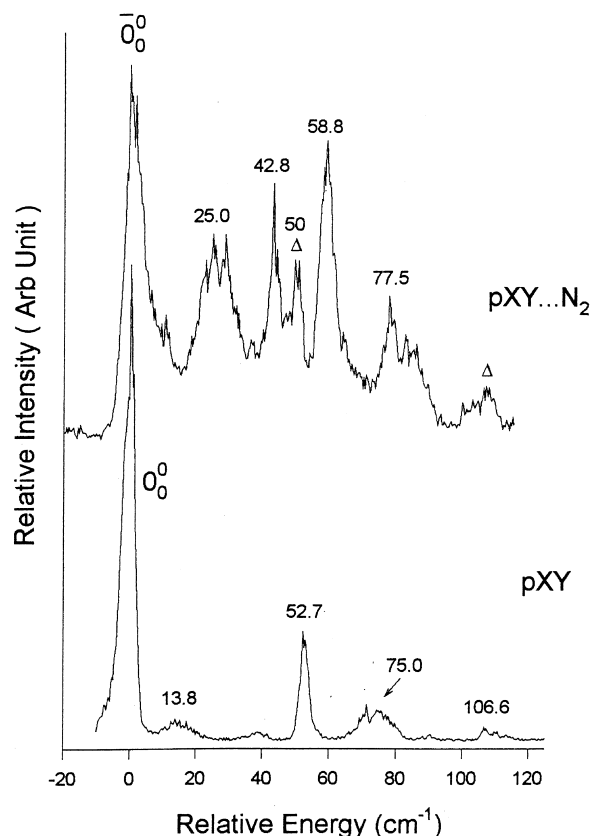


Fig. 4. R2PI spectra of *p*- $C_6H_4(CH_3)_2...N_2$ and *p*- $C_6H_4(CH_3)_2$ in the vicinity of the $S_1 \leftarrow S_0 0_0^0$ band.

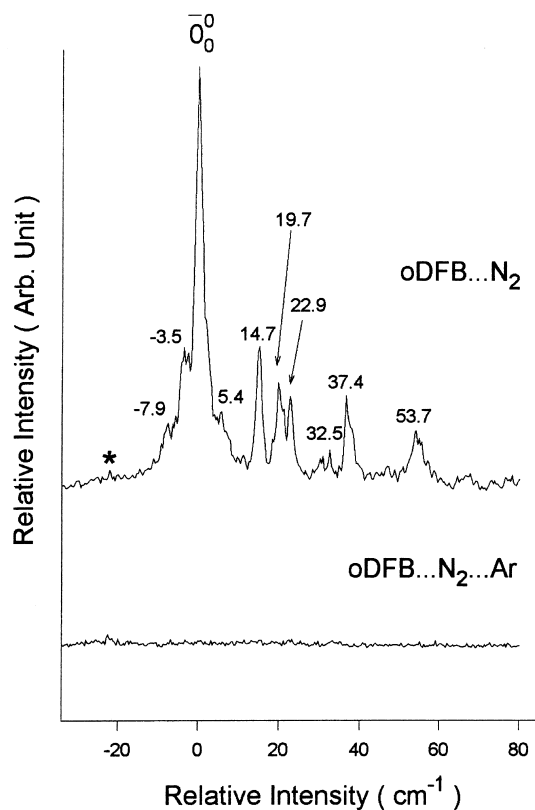


Fig. 5. R2PI spectra of $o\text{-C}_6\text{H}_4\text{F}_2 \dots \text{N}_2$ and $o\text{-C}_6\text{H}_4\text{F}_2 \dots \text{N}_2\text{Ar}$ in the vicinity of the $S_1 \leftarrow S_0$ 0_0^0 band.

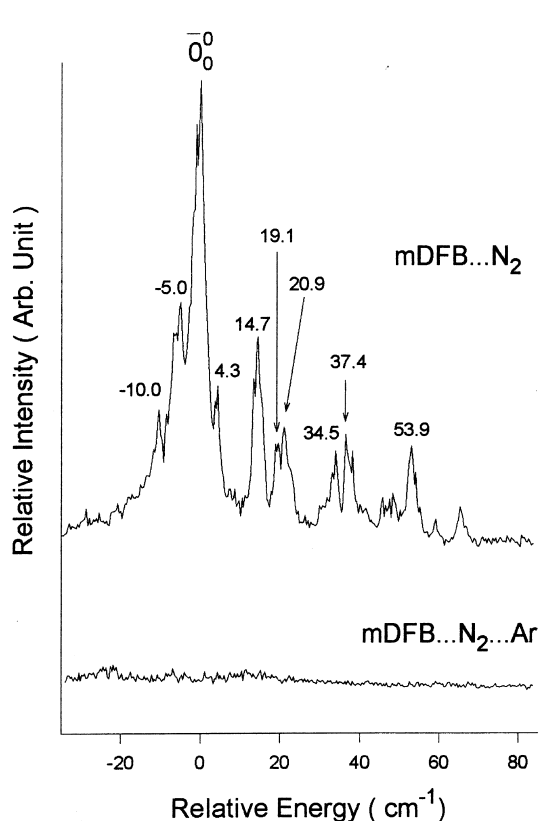


Fig. 6. R2PI spectra of $m\text{-C}_6\text{H}_4\text{F}_2 \dots \text{N}_2$ and $m\text{-C}_6\text{H}_4\text{F}_2 \dots \text{N}_2\text{Ar}$ in the vicinity of the $S_1 \leftarrow S_0$ 0_0^0 band.

According to the spectral data of the vdW complexes of BDs with Ar, the stretching vibrational frequency of Ar against the benzene ring S_{20}^1 remains essentially unchanged for different BDs. This is probably due to the fact that the distance of Ar from the benzene ring remains essentially unchanged (approximately 3.5 Å) and the reduced mass of the stretching vibration satisfies the diatomic model rather well. On the basis of this model and referring to the spectrum of $\text{C}_6\text{H}_5\text{F} \dots \text{N}_2$, we expect that the stretching vibrational frequencies of $\text{C}_6\text{H}_4\text{R}_2 \dots \text{N}_2$ ($\text{R} \equiv \text{F}, \text{CH}_3$) will be close to +50 cm^{-1} relative to 0_0^0 . This is indeed observed: $o\text{-C}_6\text{H}_4\text{F}_2 \dots \text{N}_2$, +53.7 cm^{-1} ; $m\text{-C}_6\text{H}_4\text{F}_2 \dots \text{N}_2$, +53.9 cm^{-1} ; $o\text{-C}_6\text{H}_4(\text{CH}_3)_2 \dots \text{N}_2$, +53.7 cm^{-1} ; $m\text{-C}_6\text{H}_4(\text{CH}_3)_2 \dots \text{N}_2$, +54.6 cm^{-1} ; $p\text{-C}_6\text{H}_4(\text{CH}_3)_2 \dots \text{N}_2$, 58.5 cm^{-1} . The last value exhibits a relatively large deviation from 50 cm^{-1} and is discussed below.

Of the vdW complexes, $\text{C}_6\text{H}_4\text{R}_2 \dots \text{N}_2$ ($\text{R} \equiv \text{F}, \text{CH}_3$), the vdW vibrational spectrum of $o\text{-C}_6\text{H}_4(\text{CH}_3)_2 \dots \text{N}_2$ near 0_0^0 is the simplest (see Fig. 2); it has four characteristic peaks: +23.7 cm^{-1} , +34.0 cm^{-1} , +44.6 cm^{-1} and +53.7 cm^{-1} . There are two reasons for this:

1. in the range 0–70 cm^{-1} , there is no corresponding CH_3 internal rotational transition for $o\text{-C}_6\text{H}_4(\text{CH}_3)_2 \dots \text{N}_2$;
2. in comparison with the spectrum of $o\text{-C}_6\text{H}_4(\text{CH}_3)_2 \dots \text{Ar}$ [23], it appears that there is no internal rotational transition involving N_2 .

Since the fundamental bending vibrational transition in the symmetry plane is Franck–Condon allowed, we attribute the

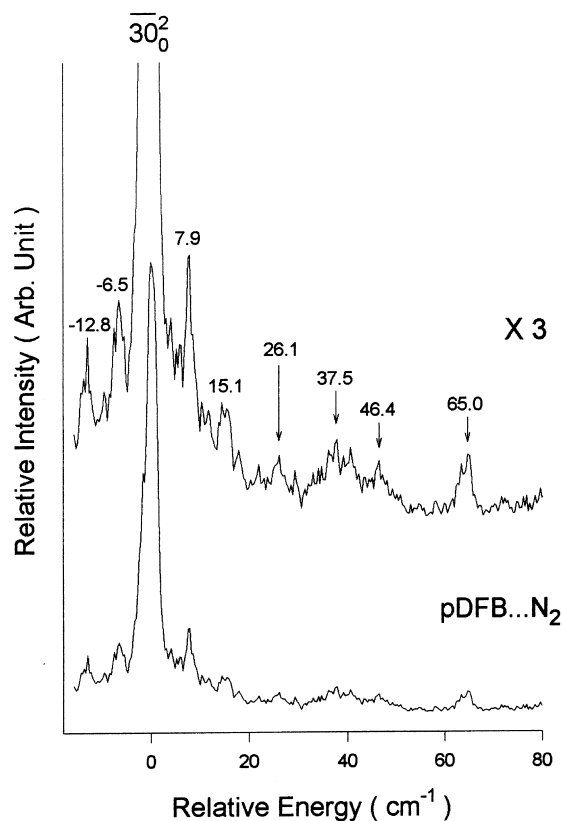


Fig. 7. R2PI spectrum of $p\text{-C}_6\text{H}_4\text{F}_2 \dots \text{N}_2$ in the vicinity of the $S_1 \leftarrow S_0$ 30_0^2 band.

Table 2

Spectra and assignment of $\text{C}_6\text{H}_4(\text{CH}_3)_2\cdots\text{N}_2$

$o\text{-C}_6\text{H}_4(\text{CH}_3)_2\cdots\text{N}_2^{\text{a,b}}$		$m\text{-C}_6\text{H}_4(\text{CH}_3)_2\cdots\text{N}_2^{\text{a,b}}$		$p\text{-C}_6\text{H}_4(\text{CH}_3)_2\cdots\text{N}_2^{\text{a,b}}$	
Band	Assignment	Band	Assignment	Band	Assignment
+23.7	$\text{b}_{x_0}^1$	+21.6	$\text{b}_{x_0}^1$	+25.0	$\text{b}_{x_0}^1$
+34.0	$\text{b}_{y_0}^1$	+30–40	(CH_3 rotation, $\text{b}_{x_0}^2$, $\text{b}_{y_0}^1$)	+42.8	$\text{b}_{y_0}^1$
+44.6	$\text{b}_{x_0}^2$	+54.6	$\text{S}_{z_0}^1$	+50.0 ^c	(CH_3 rotation)
+53.7	$\text{S}_{z_0}^1$	+73.0	(CH_3 rotation)	+58.8 ^c	$\text{S}_{z_0}^1$
+62–72	($\text{b}_{x_0}^3$, $\text{b}_{y_0}^2$, $\text{b}_{x_0}^1$, $\text{S}_{z_0}^1$)				

^a $\bar{\nu}_0$ shifts ($\Delta\nu$): –17.5 cm^{-1} (ortho); –12.0 cm^{-1} (meta); –57.5 cm^{-1} (para).^bThe band position in the table is relative to the $\bar{\nu}_0$ transition and the unit is cm^{-1} .^cFermi resonance.

peak at +23.7 cm^{-1} to $\text{b}_{x_0}^1$ and that at +44.6 cm^{-1} to $\text{b}_{x_0}^2$. Based on the spectral assignment of $\text{C}_6\text{H}_5\text{F}\cdots\text{N}_2$ (+39.3 cm^{-1} , $\text{b}_{y_0}^1$), we believe that the peak at +34 cm^{-1} is due to the fundamental bending vibrational transition perpendicular to the symmetry plane $\text{b}_{y_0}^1$. The peak at +53.7 cm^{-1} has been assigned to $\text{S}_{z_0}^1$ as discussed above.

By comparing the $\bar{\nu}_0$ band spectrum of $m\text{-C}_6\text{H}_4(\text{CH}_3)_2\cdots\text{N}_2$ with that of the monomer $m\text{-C}_6\text{H}_4(\text{CH}_3)_2$, it can be seen that the peaks at +21.6 cm^{-1} and +54.6 cm^{-1} clearly originate from the vdW vibration of N_2 relative to the benzene ring. The peak at +21.6 cm^{-1} should be due to the bending vibration of N_2 in the symmetry plane $\text{b}_{x_0}^1$, whereas the peak at +54.6 cm^{-1} should be associated with the stretching vibration $\text{S}_{z_0}^1$. A broad peak appears between +30 cm^{-1} and +40 cm^{-1} , which is probably due to the superposition of the CH_3 internal rotation and N_2 bending vibration ($\text{b}_{x_0}^2$, $\text{b}_{y_0}^1$). From the spectrum recorded, there is no clear indication of the internal rotation of N_2 .

By comparing the spectrum of $p\text{-C}_6\text{H}_4(\text{CH}_3)_2\cdots\text{N}_2$ with that of the monomer $p\text{-C}_6\text{H}_4(\text{CH}_3)_2$, we can assign the peaks corresponding to the intermolecular modes. In the vicinity of the origin $\bar{\nu}_0$ of $p\text{-C}_6\text{H}_4(\text{CH}_3)_2$ (0–70 cm^{-1}), the monomer spectrum has only one peak (52.7 cm^{-1}) involving transitions between the internal rotational levels of the methyl groups, whereas in the same region relative to $\bar{\nu}_0$, $p\text{-C}_6\text{H}_4(\text{CH}_3)_2\cdots\text{N}_2$ shows four peaks (25.0 cm^{-1} , 42.8 cm^{-1} , 50.0 cm^{-1} and 58.8 cm^{-1}). In the spectral region above 70 cm^{-1} relative to the origin peaks, the spectra of the monomer and complex show a one-to-one correspondence. Since in the range 0–70 cm^{-1} , the peak of $p\text{-C}_6\text{H}_4(\text{CH}_3)_2\cdots\text{N}_2$ at 50.0 cm^{-1} has a similar position and shape to the peak of the monomer at 52.7 cm^{-1} , we attribute it to the transition between the methyl internal rotational levels of the methyl groups. Therefore the remaining peaks of the complex are due to the excitation of the intermolecular vibrational modes. By analogy with the spectral assignments of other complexes in the literature, we attribute the peak at 58.8 cm^{-1} to the stretching motion $\text{S}_{z_0}^1$ of N_2 perpendicular to the benzene ring. It is interesting to note that this value (58.8 cm^{-1}) is significantly larger than those of the stretching motion $\text{S}_{z_0}^1$ of o - and $m\text{-C}_6\text{H}_4(\text{CH}_3)_2\cdots\text{N}_2$ which are both around 53–55 cm^{-1} .

The fact that the peak due to methyl rotation is red shifted relative to that of the monomer and the peak corresponding to the stretching mode is blue shifted relative to that of the ortho- and meta-substituted complexes points forcefully to a strong interaction (Fermi resonance) between the CH_3 internal rotational level and the fundamental energy level of the vdW stretching mode. Such Fermi resonance between the methyl rotational level and vdW vibrational modes has been reported for $\text{C}_6\text{H}_5\text{CH}_3\cdots\text{Ar}$ [7]. According to our assignments for o - and $m\text{-C}_6\text{H}_4(\text{CH}_3)_2$ above and our previous work on $\text{C}_6\text{H}_5\text{F}\cdots\text{N}_2$, we believe that the peak at 25.0 cm^{-1} is due to the fundamental excitation $\text{b}_{x_0}^1$ of the bending motion of N_2 along the direction defined by the two methyl groups, and the peak at 42.8 cm^{-1} corresponds to the fundamental excitation $\text{b}_{y_0}^1$ of the bending motion of N_2 perpendicular to the direction defined by the two methyl groups. These two transitions which excite the fundamental vibration of the two modes are not Franck–Condon allowed, but rather originate from the coupling of the electronic states and the vdW bending modes. The overall assignment is listed in Table 2.

If we compare the $3\bar{\nu}_0^2$ band spectrum of $p\text{-C}_6\text{H}_4\text{F}_2\cdots\text{N}_2$ and the $\bar{\nu}_0$ band spectra of $o\text{-C}_6\text{H}_4\text{F}_2\cdots\text{N}_2$ and $m\text{-C}_6\text{H}_4\text{F}_2\cdots\text{N}_2$ with the corresponding band spectra of $p\text{-C}_6\text{H}_4\text{F}_2\cdots\text{Ar}$ [18], $o\text{-C}_6\text{H}_4\text{F}_2\cdots\text{Ar}$ [24] and $m\text{-C}_6\text{H}_4\text{F}_2\cdots\text{Ar}$ [24], we find that the spectrum of $\text{C}_6\text{H}_4\text{F}_2\cdots\text{N}_2$ is more complicated than that of $\text{C}_6\text{H}_4\text{F}_2\cdots\text{Ar}$. We believe that the complexity of the former spectrum originates from the internal rotation of N_2 above the benzene ring in addition to the vdW vibrational modes (a tentative assignment is listed in Table 3). We have recently discussed the internal rotation of $\text{C}_6\text{H}_5\text{X}\cdots\text{N}_2$ ($\text{X} \equiv \text{F}, \text{Cl}, \text{Br}$) in some detail. The symmetry group of the vdW complexes $\text{C}_6\text{H}_5\text{X}\cdots\text{N}_2$ is G_4 . The internal rotational barrier is estimated on the basis of fitting to the potential $U(\theta) = U_2(1 - \cos 2\theta)$, solving a one-dimensional Schrodinger equation and obtaining the internal rotational energy level as a function of the barrier U_2 . From this, we successfully assigned the internal rotational transitions of $\text{C}_6\text{H}_5\text{X}\cdots\text{N}_2$ [11]. For the three conformers of $\text{C}_6\text{H}_4\text{F}_2\cdots\text{N}_2$, considering the internal rotation of N_2 , the symmetry group of $o\text{-C}_6\text{H}_4\text{F}_2\cdots\text{N}_2$ and $m\text{-C}_6\text{H}_4\text{F}_2\cdots\text{N}_2$ is G_4 and that of $p\text{-C}_6\text{H}_4\text{F}_2\cdots\text{N}_2$ is G_8 . The character table of the irreducible representation of G_8 is given

Table 3
Spectra and assignment of $C_6H_4F_2...N_2$

$o-C_6H_4F_2...N_2^{a,c}$			$m-C_6H_4F_2...N_2^{a,c}$			$p-C_6H_4F_2...N_2^{a,b,c}$		
Band	Assignment	Calculated	Band	Assignment	Calculated	Band	Assignment	Calculated
–7.9	$2a_1 \rightarrow 0a_1$	–8.7	–10.0	$2a_1 \rightarrow 0a_1$	–8.9	–12.8	$2a'_1 \rightarrow 0a'_1$	–12.0
–3.5	$1b_2 \rightarrow 1a_2$	–3.3	–5.0	$1b_2 \rightarrow 1a_2$	–4.2	–6.5	$1b''_2 \rightarrow 1b''_1$	–6.5
+5.4	$1b_2 \rightarrow 1b_2$	+5.5	+4.3	$1b_2 \rightarrow 1b_2$	+4.6	+7.9	$1b''_1 \rightarrow 1b''_2$	+8.4
+14.7	$0a_1 \rightarrow 2a_1$	+14.9	+14.7	$0a_1 \rightarrow 2a_1$	+14.9	+15.1	$0a'_1 \rightarrow 2a'_1$	+14.9
+19.7	b_{y0}^1		+19.1	b_{x0}^1		+26.1	$\overline{30_0^2} b_{x0}^1$	
+22.9	$1a_2 \rightarrow 3a_2$	+21.4	+20.9	$1a_2 \rightarrow 3a_2$	+21.5	+37.5	$\overline{30_0^2} b_{y0}^1$	
+32.5	b_{y0}^1		+34.5	b_{y0}^1		+46.4	$\overline{30_0^2} S_{z0}^1$	
+37.4	b_{x0}^2		+37.4	b_{x0}^2		+65.0	$\overline{30_0^2} b_{y0}^2$	
+53.7	S_{z0}^1		+53.9	S_{z0}^1				
			+65.4	b_{y0}^2				

^a $\bar{0}_0^0$ shift ($\Delta\nu$): –13.6 cm^{-1} (ortho); –11.4 cm^{-1} (meta); –27.0 cm^{-1} (para).

^bThe $\bar{0}_0^0$ shift ($\Delta\nu$) of $p-C_6H_4F_2...N_2$ is taken from the fluorescence excitation spectra of Ref. [25].

^cThe band position in the table is relative to the $\bar{0}_0^0$ transition, except for $p-C_6H_4F_2...N_2$, and the unit is cm^{-1} . The band origin of $p-C_6H_4F_2...N_2$ is relative to the $\overline{30_0^2}$ transition. $U(\theta) = U_2(1 - \cos 2\theta)$, where the parameters U_2 for $o-C_6H_4F_2...N_2$ are 5 cm^{-1} (S_0 state) and 19 cm^{-1} (S_1 state), for $m-C_6H_4F_2...N_2$ are 7 cm^{-1} (S_0 state) and 19 cm^{-1} (S_1 state) and for $p-C_6H_4F_2...N_2$ are 13 cm^{-1} (S_0 state) and 19 cm^{-1} (S_1 state).

in Table 4 and that of G_4 can be found in Ref. [11]. Clearly, the internal rotational barrier of $C_6H_4F_2...N_2$ can still be expressed as $U(\theta) = U_2(1 - \cos 2\theta)$, and the relationship between the internal rotational energy levels and U_2 described in Ref. [11] can be used for the complex $C_6H_4F_2...N_2$. For the molecular symmetry groups G_4 and G_8 , the internal rotational wavefunctions are (a_1, a_2, b_1, b_2) and $(a'_1, a'_2, b''_1, b''_2)$ respectively. For the electronic transition $S_1 \leftarrow S_0$ of $C_6H_4F_2...N_2$, the molecular symmetry readily gives the internal rotational selection rule for o - and m - $C_6H_4F_2...N_2$ as: $a_1 \leftrightarrow a_1, b_1 \leftrightarrow b_1, a_2 \leftrightarrow a_2, b_2 \leftrightarrow b_2, a_1 \leftrightarrow b_1, a_2 \leftrightarrow b_2, a_1 \leftrightarrow a_2, a_1 \leftrightarrow b_2, b_1 \leftrightarrow a_2$ and $b_1 \leftrightarrow b_2$. The internal rotational selection rule for the electronic transition $S_1 \leftarrow S_0$ of p - $C_6H_4F_2...N_2$ can be derived as: $a'_1 \leftrightarrow a'_1, a'_2 \leftrightarrow a'_2, b''_1 \leftrightarrow b''_1, b''_2 \leftrightarrow b''_2, a'_1 \leftrightarrow a'_2, b''_1 \leftrightarrow b''_2, a'_1 \leftrightarrow b''_1, a'_1 \leftrightarrow b''_2, a'_2 \leftrightarrow b''_1$ and $a'_2 \leftrightarrow b''_2$. For o -, m - and p - $C_6H_4F_2...N_2$, if we choose U_2 of the ground electronic state (S_0) to be 5 cm^{-1} , 7 cm^{-1} and 13 cm^{-1} respectively and that of the excited state (S_1) to be 19 cm^{-1} , all the spectral lines near $\bar{0}_0^0$ or $\overline{30_0^2}$, except the peaks which were assigned to the vdW vibrations discussed above, can be assigned to internal rotational transitions as listed in Table 3.

It should be pointed out that the above assignments are tentative, and further confirmation is need using techniques such as dispersed fluorescence, hole-burning spectroscopy, etc.

4.2. Line shift of the $\bar{0}_0^0$ band

It can be seen from Tables 2 and 3 that the $\bar{0}_0^0$ band transition frequencies of all the vdW complexes studied, i.e. o -, m - and p - $C_6H_4R_2...N_2$, are red shifted ($\Delta\nu < 0$) relative to those of the $\bar{0}_0^0$ band of o -, m - and p - $C_6H_4R_2...N_2$. This suggests that the vdW binding energies are larger in the excited state S_1 than in the ground state S_0 .

Previous studies have shown that the $\bar{0}_0^0$ band shift $\Delta\nu$ of

$C_6H_5F...N_2$ is –14.0 cm^{-1} [11]. In another experiment, we found that the $\Delta\nu$ value of the $\bar{0}_0^0$ band of $C_6H_5CH_3...N_2$ was –28.5 cm^{-1} . As shown in Tables 2 and 3, the $\bar{0}_0^0$ band shifts $\Delta\nu$ of p - $C_6H_4F_2...N_2$ and p - $C_6H_4(CH_3)_2$ are –27.0 cm^{-1} and –57.5 cm^{-1} respectively, double the values of the corresponding mono-substituted complexes. This is by no means a coincidence, but rather implies that, when the substituents are in the para position, their contributions to the change in the vdW interaction potential energy between S_0 and S_1 are additive, a phenomenon which can be explained by the Lennard–Jones atom–atom interaction potential. Also evident from Tables 2 and 3 is that of o -, m - and p - $C_6H_4F_2...N_2$ and o -, m - and p - $C_6H_4(CH_3)_2...N_2$, p - $C_6H_4R_2...N_2$ has the largest $\Delta\nu$ value, m - $C_6H_4R_2...N_2$ has the smallest $\Delta\nu$ value and o - $C_6H_4R_2...N_2$ has an intermediate $\Delta\nu$ value. It appears from the above discussion that the $\bar{0}_0^0$ band shift $\Delta\nu$ is influenced by two factors: the number of substituents and the relative positions of the substituents. This is similar to the $\bar{0}_0^0$ band shifts of BDs relative to the $\bar{0}_0^0$ band of benzene [26].

The large difference in the $\bar{0}_0^0$ band shifts between p - $C_6H_4F_2...N_2$ and p - $C_6H_4(CH_3)_2...N_2$ merits discussion. The fact that $\Delta\nu(\bar{0}_0^0)$ of p - $C_6H_4F_2...N_2$ is about half that of p - $C_6H_4(CH_3)_2...N_2$ can be explained by the dispersion interaction term in the vdW interaction potential. Since the dispersion interaction potential is directly proportional to the polarizability, the change in the vdW interaction energy from S_0 to S_1 should be proportional to the change in the polarizabilities of the two electronic states, i.e.

$$\Delta\nu_F/\Delta\nu_{CH_3} = \Delta E_F/\Delta E_{CH_3} \sim \Delta\alpha_F/\Delta\alpha_{CH_3} \quad (2)$$

The polarizabilities of S_1 (α^*) and S_0 (α_0) have the following approximate relationship [27]

$$\alpha^*/\alpha_0 = I_0/I^* = I_0/(I_0 - E^*) \quad (3)$$

where I^* and I_0 are the ionization potentials of the complexes in the S_1 and S_0 states respectively and E^* is the excitation

Table 4
Character table of group G_8

G_8	E	$(1,3)(2,4)(5,6)$	$(2,3)(1,4)^*$	$(1,2)(3,4)(5,6)^*$	$(7,8)$	$(1,3)(2,4)(5,6)(7,8)$	$(2,3)(1,4)(7,8)^*$	$(1,2)(3,4)(5,6)(7,8)^*$
Int. rot.	θ	$\pi + \theta$	$2\pi - \theta$	$\pi - \theta$	$\pi + \theta$	θ	$\pi - \theta$	$2\pi - \theta$
Equi. rot.	R_z^0	R_z^0	R_y^0	R_x^0	R_z^0	R_z^0	R_y^0	R_x^0
A'_1	1	1	1	1	1	1	1	1
A'_2	1	1	1	1	1	1	1	1
B'_1	1	1	1	1	1	1	1	1
B'_2	1	1	1	1	1	1	1	1
A''_1	1	1	1	1	1	1	1	1
A''_2	1	1	1	1	1	1	1	1
B''_1	1	1	1	1	1	1	1	1
B''_2	1	1	1	1	1	1	1	1

energy from S_0 to S_1 . The change in polarizability from S_0 to S_1 is therefore

$$\Delta\alpha = \alpha^* - \alpha_0 = E^* / (I_0 - E^*) \quad (4)$$

The ionization potentials of $p\text{-C}_6\text{H}_4\text{F}_2\ldots\text{N}_2$ and $p\text{-C}_6\text{H}_4(\text{CH}_3)_2\ldots\text{N}_2$ are found from Ref. [28] to be 9.14 eV and 8.44 eV respectively and the ground state polarizabilities are 10.3 \AA^3 and 14.9 \AA^3 respectively. The S_1 electronic transition energies of the two complexes are 4.565 eV and 4.553 eV respectively. Substituting the I , E and α values into Eq. (2), we obtain the ratio in Eq. (3) to be 0.59. This value is close to the ratio of $\Delta\nu(\bar{\nu}_0^0)$ of the two complexes (0.47). This indicates that, on electronic excitation from S_0 to S_1 , the change in vdW interaction energy is dominated by the dispersion interaction term.

As can be seen from Tables 2 and 3, the $\bar{\nu}_0^0$ band shifts of o - and m - $\text{C}_6\text{H}_4\text{R}_2\ldots\text{N}_2$ ($\text{R} \equiv \text{F}, \text{CH}_3$) are close, but different from those of p - $\text{C}_6\text{H}_4\text{R}_2\ldots\text{N}_2$ ($\text{R} \equiv \text{F}, \text{CH}_3$). This difference in line shift may be attributed to the different electrostatic interactions between the dipole moments of the three isomeric $\text{C}_6\text{H}_4\text{R}_2\ldots\text{N}_2$ ($\text{R} \equiv \text{F}, \text{CH}_3$) compounds and the quadrupole moment of N_2 . While the dipole moment of p - $\text{C}_6\text{H}_4\text{R}_2\ldots\text{N}_2$ ($\text{R} \equiv \text{F}, \text{CH}_3$) is zero, o - and m - $\text{C}_6\text{H}_4\text{R}_2\ldots\text{N}_2$ ($\text{R} \equiv \text{F}, \text{CH}_3$) have dipole moments around 1 D [28]. Conceivably, during the electronic transition $S_1 \leftarrow S_0$, the change in vdW interaction mainly stems from the dispersion term for p - $\text{C}_6\text{H}_4\text{R}_2\ldots\text{N}_2$ ($\text{R} \equiv \text{F}, \text{CH}_3$). For o - and m - $\text{C}_6\text{H}_4\text{R}_2\ldots\text{N}_2$ ($\text{R} \equiv \text{F}, \text{CH}_3$), however, the change in vdW interaction during the $S_1 \leftarrow S_0$ transition should include not only the dispersion term but also the quadrupole–dipole interaction term. In addition, the relative positions of the methyl groups can affect their conformations [29] which, in turn, can affect the interaction between the aromatic molecule and N_2 . This is probably one of the sources of the different $\bar{\nu}_0^0$ band shifts of o -, m - and p - $\text{C}_6\text{H}_4\text{R}_2\ldots\text{N}_2$ ($\text{R} \equiv \text{F}, \text{CH}_3$).

5. Conclusions

We have studied the excitation spectra of o -, m - and p - $\text{C}_6\text{H}_4\text{R}_2\ldots\text{N}_2$ ($\text{R} \equiv \text{F}, \text{CH}_3$) in the vicinity of the $S_1 \leftarrow S_0$ $\bar{\nu}_0^0$ band using supersonic beam and multiphoton ionization techniques. Several conclusions can be drawn from our spectral analysis.

1. N_2 in o -, m - and p - $\text{C}_6\text{H}_4\text{F}_2\ldots\text{N}_2$ rotates almost freely around the axis perpendicular to the benzene ring with a barrier of 19 cm^{-1} in S_1 and $5\text{--}13 \text{ cm}^{-1}$ in S_0 .
2. For o -, m - and p - $\text{C}_6\text{H}_4(\text{CH}_3)_2\ldots\text{N}_2$, no spectral features associated with the excitation of the internal rotations of N_2 were observed.
3. For o - and m - $\text{C}_6\text{H}_4\text{R}_2\ldots\text{N}_2$ ($\text{R} \equiv \text{F}, \text{CH}_3$), the vdW stretching vibrational frequency of N_2 perpendicular to the benzene ring is $53\text{--}55 \text{ cm}^{-1}$, the in-plane bending frequency is $19\text{--}23 \text{ cm}^{-1}$ and the bending frequency perpendicular

to the symmetry plane is $32\text{--}35\text{ cm}^{-1}$. The situation for $p\text{-C}_6\text{H}_4\text{R}_2\cdots\text{N}_2$ ($\text{R}\equiv\text{F}$, CH_3) is quite different presumably due to the higher symmetry. In addition, Fermi resonance has been observed for $p\text{-C}_6\text{H}_4(\text{CH}_3)_2\cdots\text{N}_2$ between the CH_3 internal rotational levels and the vdW stretching motion of N_2 against the benzene ring.

4. For all the complexes studied, i.e. *o*-, *m*- and *p*- $\text{C}_6\text{H}_4\text{R}_2\cdots\text{N}_2$, irrespective of whether $\text{R}\equiv\text{F}$ or CH_3 , the $\tilde{0}_0^0$ band shifts relative to the monomer origins $\tilde{0}_0^0$ are largest for the para-substituted complexes, least for the meta-substituted complexes and in between for the ortho-substituted complexes. Therefore the $\tilde{0}_0^0$ band shift depends not only on the number of R species, but also on the relative positions of the R species. By comparing the magnitude of the band shift of $p\text{-C}_6\text{H}_4(\text{CH}_3)_2\cdots\text{N}_2$ with that of $p\text{-C}_6\text{H}_4\text{F}_2\cdots\text{N}_2$, it was found that the ratio of the band shifts is, to a good approximation, directly proportional to the ratio of the monomer polarizability changes from S_0 to S_1 , suggesting that the band shifts mainly originate from the change in the dispersion interaction term of the vdW potential on electronic excitation.

Acknowledgements

This work was supported by an RGC Grant (HKUST204/93E) administered by the UGC of Hong Kong.

References

- [1] R. Nowak, J.A. Menapace, E.R. Bernstein, J. Chem. Phys. 89 (1988) 1309.
- [2] J.A. Menapace, E.R. Bernstein, J. Phys. Chem. 91 (1987) 2533.
- [3] Th. Weber, A. von Bargaen, E. Riedle, H.J. Neusser, J. Chem. Phys. 92 (1990) 90.
- [4] A.J. Gotch, T.S. Zwier, J. Chem. Phys. 93 (1990) 6977; 96 (1992) 3388.
- [5] A.W. Garrett, T.S. Zwier, J. Chem. Phys. 96 (1992) 3402.
- [6] E.J. Bieske, M.W. Rainbird, L.M. Atkinson, A.E.W. Knight, J. Chem. Phys. 91 (1989) 752.
- [7] M. Mons, J. Le Calve, F. Piuze, U. Dimicoli, J. Chem. Phys. 92 (1990) 2155.
- [8] M. Mons, J. Le Calve, Chem. Phys. 146 (1990) 195.
- [9] R. Disselkamp, E.R. Bernstein, J. Chem. Phys. 98 (1993) 4339.
- [10] S. Sun, E.R. Bernstein, J. Chem. Phys. 103 (1995) 4447.
- [11] Y.H. Hu, W.Y. Lu, S.H. Yang, J. Chem. Phys. 105 (1996) 5305.
- [12] W.Y. Lu, Y.H. Hu, S.H. Yang, J. Chem. Phys. 104 (1996) 8843. R.B. Huang, W.Y. Lu, S.H. Yang, J. Chem. Phys. 102 (1995) 189. W.Y. Lu, R.B. Huang, S.H. Yang, J. Phys. Chem. 99 (1995) 12 099. W.Y. Lu, R.B. Huang, S.H. Yang, Chem. Phys. Lett. 241 (1995) 373.
- [13] J. Wana, E.R. Bernstein, J. Chem. Phys. 84 (1986) 928.
- [14] D.E. Williams, S.R. Cox, Acta Crystallogr. Sect. B 40 (1984) 404.
- [15] Y. Ohshima, H. Kohguchi, Y. Endo, Chem. Lett. 184 (1991) 21.
- [16] P. Hobza, O. Bludsky, H. Selzle, E.W. Schlag, J. Chem. Phys. 98 (1993) 6223.
- [17] R. Sussmann, R. Neuhauser, H.J. Neusser, J. Chem. Phys. 103 (1995) 3315.
- [18] R. Sussmann, H.J. Neusser, J. Chem. Phys. 102 (1995) 3055.
- [19] P.M. Maxton, M.W. Schaeffer, S.M. Ohline, W. Kim, V.A. Venturo, P.M. Felker, J. Chem. Phys. 101 (1994) 8391.
- [20] S. Martrenchard, C. Jouviet, C. Lardeux-Dedonder, D. Solgadi, J. Phys. Chem. 95 (1991) 9186.
- [21] Y. Tsuchiya, K. Takazawa, M. Fujii, M. Ito, Chem. Phys. Lett. 183 (1991) 107.
- [22] P.J. Breen, J.A. Warren, E.R. Bernstein, J. Chem. Phys. 87 (1987) 1917.
- [23] T. Droz, S. Leutwyler, M. Mandziuk, Z. Bacic, J. Chem. Phys. 101 (1994) 6412.
- [24] W.Y. Lu, Y.H. Hu, S.H. Yang, in preparation.
- [25] B.D. Gibert, C.S. Parmenter, J. Phys. Chem. 99 (1995) 2444.
- [26] J. Petruska, J. Chem. Phys. 34 (1961) 1111, 1120.
- [27] H.-Y. Kim, M.W. Cole, J. Chem. Phys. 90 (1989) 6055.
- [28] R.L. David, Handbook of Chemistry and Physics, CRC, London, 75th Ed., 1995.
- [29] K. Okuyama, N. Mikami, M. Ito, J. Phys. Chem. 89 (1985) 5617.